Evolution of Composition and Methane Occurrence of Bituminous Coal after Igneous Intrusion: A Case Study of Daxing Coal Mine, Tiefa Basin, China

Yiming Huang, Jingyu Jiang,* Yuanping Cheng, Huazhou Huang, and Lei Zhang

Read Online

ACCESS | Metrics & More | Article Recommendations

ABSTRACT: Since 1987, there have been 10 coal and gas outbursts in Daxing Coal Mine, Tiefa Basin. It was reported that these outbursts were related to igneous intrusion. To study the influence of igneous intrusion into bituminous on coal bed methane (CBM) occurrence, eight coal samples were collected at different distances (0.2−10 m) from an intrusion in Daxing Coal Mine. The petrographic and chemical data, pore characteristics, and adsorption properties of unaltered and heat-affected coals were tested and compared. Approaching the dike, vitrinite reflectance (R_o) increases from 0.56 to 1.14%, while moisture decreases from 6.4 to 3.1%. According to R_o, with the thermal evolution of igneous rocks, the temperature of heat-affected coal seams generally increases from ~78 to ~169 °C. The bituminous coal contained high moisture content before the intrusion, and after the igneous intrusion, partial heat may be used for moisture gasification; the other heat was used to improve coal metamorphism, resulting in little increase in the coal metamorphism as expected. The synergistic effect of igneous thermal evolution and moisture content change improves the adsorption capacity of coal. Affected by the igneous intrusion, the gas content of the heat-affected coal seams No. 4 (above the sill) and No. 7 (below the sill) is higher than that of the unaltered No. 12 coal seam, and the gas content of No. 7 coal seam (beneath the sill) is higher than that of No. 4 coal seam. The low permeability sill has a sealing effect on the gas in No. 7 coal seam. Therefore, the evolution process of CBM occurrence in the Daxing Coal Mine can be speculated, that is, after magma intrusion, the temperature increased, the metamorphic degree of coal increased, and water gasification occurred at the same time. The original adsorption site occupied by moisture was vacated, which improved the methane adsorption capacity of the coal and provided favorable conditions for CBM occurrence.
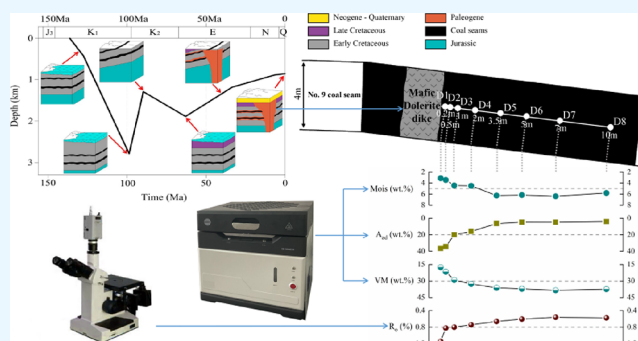
1. INTRODUCTION

With the exploitation of coal resources, the conditions encountered in the mining process of coal around the world are more complex and variable. Many coal bed methane (CBM) basins have undergone thermal evolution or contact metamorphism related to igneous intrusions, such as the Piceance basins in America,[1] the Bowen basins in Australia,[2,3] the Qinshui basins in China,[4] the Raniganj basins in India,[5] the Karoo basin in South Africa,[6−8] the Donets basin in Ukraine and Russia,[9] and the Sverdrup basin in Canada[10] (Table 1). Igneous intrusions have significant effects on the coal rank, petrographic properties, and the mineralogical and chemical composition of coal.[10−21] Due to the igneous intrusion, the inorganic constituents and minerals in coal have changed.[15,22] Affected by igneous intrusions, vitrinite reflectance (R_o), ash yield, fixed carbon, and carbon content of coal increase, whereas the in moisture, volatile matter (VM), nitrogen, and hydrogen content of coal decrease. Meanwhile, it causes the loss of liptinite, and the formation of nature coke, pyrolytic

carbon, and graphitized coals within the thermal aureole.[7,11,12,23] However, the synergistic effect of igneous intrusion and internal moisture change on CBM occurrence characteristics has not attracted much attention.

Dikes are important for driving hydrothermal circulation, but not for generating large volumes of methane through direct conductive heating.[16] According to the survey results of gas outburst events in the Highveld coalfields of South Africa, the sites of high gas emissions are substantially in the adjacent of the igneous intrusions. The porosity properties and adsorption capacity of the heat-affected coals have been improved, thus the CBM storage capacity has improved.[24,25] The study of the

Table 1. World-Wide Coal Basins/Coalfields Investigated for Igneous Intrusion

basin	coalfield	country	sill/dike	intrusion geological time	reference
Piceance		USA			1
	Midland Valley	Scotland	sill	Carboniferous	29
Bowen		Australia			2,3
Gunnedah		Australia	sill	Permian	17,30,31
South Sumatra		Indonesia	sill	Quaternary	32
Raton		USA	sill, dike	Cretaceous-Paleocene	16
Illinois		USA	dike	Cretaceous	11,12,33
San Juan		USA			4
Sydney		Australia		Permian to Tertiary	24,34,35
Donets		Ukraine, Russia		Permo-Triassic	9
	Jharia	Indian	sill, dike	Lower Cretaceous	36,37
Gondwana		Indian	dike	Cretaceous?	14
Raniganj		Indian	dike	Permian	5
	Handan	China	sill, dike	Permian	4,13,15
	Highveld	South Africa	sill	Jurassic	7
Karoo		South Africa	dike	Jurassic	6,8
Sverdrup		Canada	dike	Jurassic, Cretaceous	10
	Huaibei,	China	sill, dike	Jurassic, Cretaceous	4,13,28
	Hongyang	China	sill, dike	Cretaceous	4,13
	Huainan	China	sill, dike	Cretaceous	19
	Hanpo'ao	China	sill, dike	Permian, Triassic	23
Qinshui		China		Jurassic, Cretaceous	4
Fuxin		China		Tertiary	4,38
Tiefa		China	sill	Tertiary	39,40
Moatize		Mozambique	sill	Permian	41
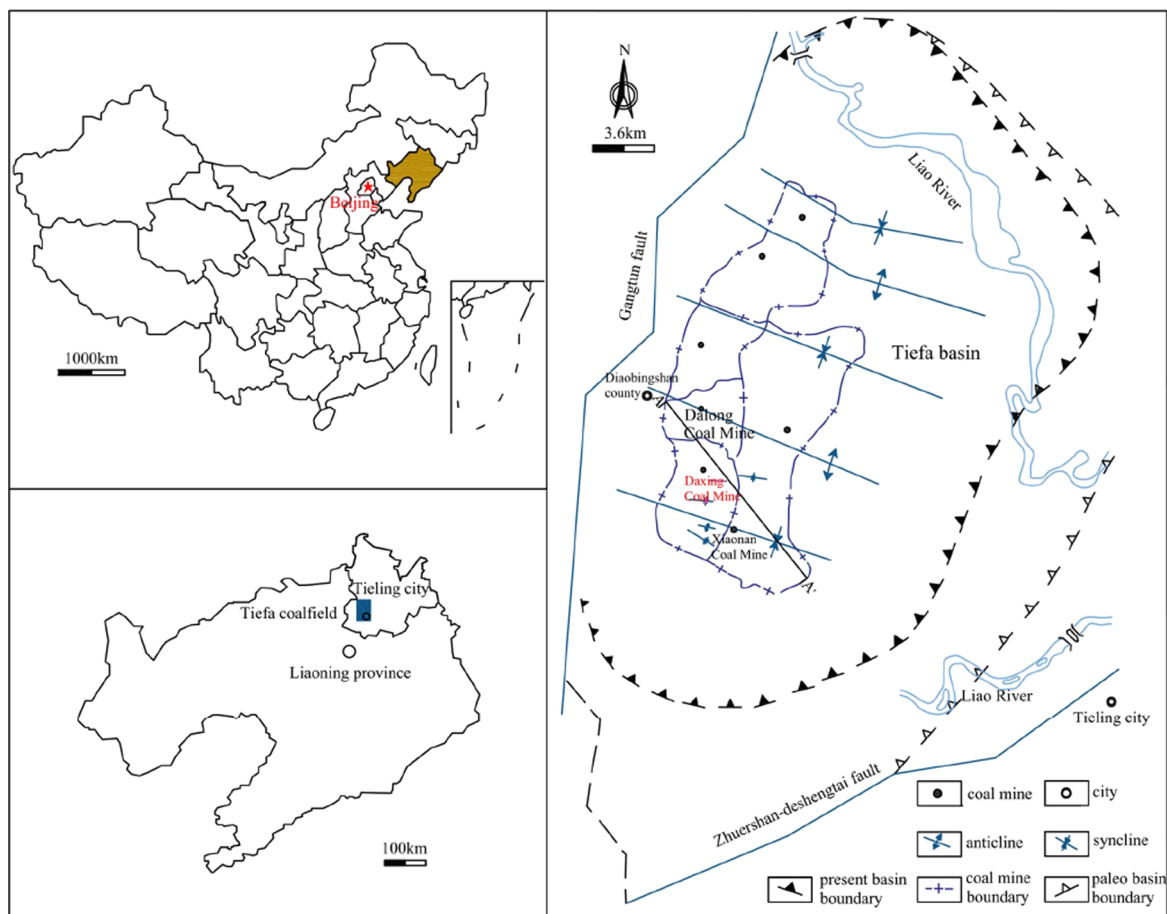
Figure 1. Map showing study area, data locations for stratigraphic characteristics, and section from Tiefa Basin (elevation of the ground is +73 m).

Hoskissons coalfield in Gunnedah basin shows that the mineralization effect is not the key factor affecting the gas flow capacity. Complex stress orientation reduces the connectivity of fractures and affects the flow characteristics of gas.[26,27] As the intrusion is closer to the coal seam, the thermal effect is more obvious. The high gas content shows the great potential of commercial development of CBM. On the other aspect, it also indicates a serious safety problem in coal mines.[9] In the process of coal mining, igneous intrusions can cause coal and gas outburst in coal mines.[7,9,28]

The influence of magma intrusion on coal seam is related to the initial temperature of magma, coal pore moisture, formation maturity before magma intrusion, and thermal conductivity of formation.[29] The remarkable characteristic of bituminous coal is high moisture.[42] After magma intrusion, the moisture in coal decreases, which destroys the competitive adsorption equilibrium of gas and water molecules in the coal matrix.[21,43] When the moisture increases from 0 to 8.5%, the macropore diffusion coefficient decreased by 82%, and the micropore diffusion coefficient decreased by 88%.[44] Therefore, it is judged that the water adsorption of coal is the key mechanism to adjust methane adsorption. Most adsorption isotherm experiments are carried out with dry coal, however, the water in coal significantly affects CBM occurrence.[45−48] As for the competitive adsorption on coal, CH_4 and CO_2 are forced to reduce the energy level in the presence of moisture.[49] The experiments showed that the invasion water can displace the adsorbed methane in the matrix micropores of coal and result in the increase of the free gas content.[50] The magma intrusion caused abnormal gas emission during coal mining in many underground coal mines. Therefore, it is necessary to study the influence of igneous intrusion and internal moisture variation on the CBM occurrence characteristics.

Since 1987, ten outbursts have occurred in Daxing Coal Mine, Tiefa Basin. It was reported that these outbursts were related to igneous intrusion. However, there is still a lack of systematic research on the influence of igneous intrusion on the CBM occurrence and adsorption characteristics of bituminous coal in Daxing Coal Mine, Tiefa Basin.

2. GEOLOGICAL SETTING

2.1. Geological Stratigraphy of Tiefa Basin. The Tiefa Basin is a continental sedimentary basin[39] and one of the main coal mining areas in Northeast China, located in Tieling City, Liaoning Province, China. The map of the study area, data locations for stratigraphic characteristics, and profile from Tiefa Basin are shown in Figure 1. The minerable coal seams are Nos. 2, 4, 7, 9, 12, 13, 15, and 16, respectively. The stratigraphic column of the Daxing Coal Mine is shown in Figure 2. The bedrock of the Tiefa Basin is composed of Cretaceous basal beds of continental sedimentary strata and quaternary sediments. The coal-bearing units are the Fuxin group of the lower Cretaceous, and the four lithologic members of this group, respectively, are: the glutenite section (K_1f_1), the lower coal-bearing member (K_1f_2), the sand−mudstone member (K_1f_3), and the top coal-bearing member (K_1f_4). The coal seams are staggered with other geological units (including mudstones, shales, or clays).CBM is extracted from the lower coal-bearing segment (K_1f_2) and the top coal-bearing segment (K_1f_4).

There are three stages of igneous activity in the Tiefa Basin. The first and second stages were dominated by eruptive rock. At the third stage, Himalayan (36.5−53 Ma) exhibited igneous
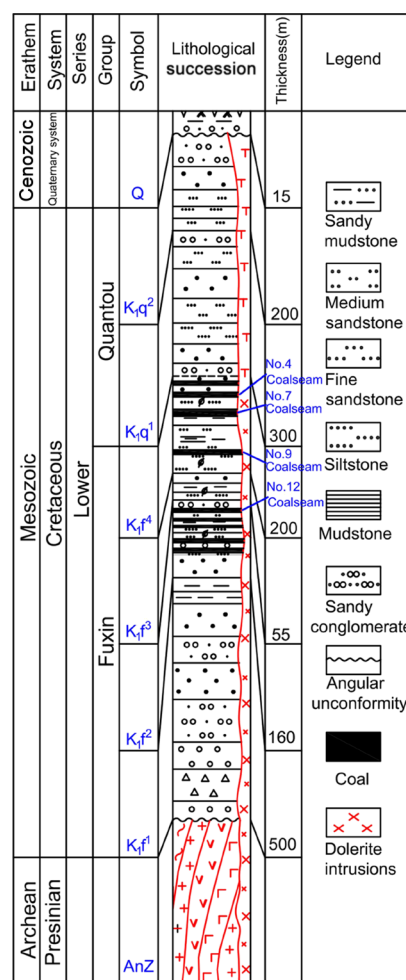
Figure 2. Stratigraphic column of Daxing Coal Mine.

activity mainly by intrusive rocks. The lithology of igneous rock is diabase, rich in iron and magnesium. The deep magma upwelled along the Gangtun fault and invaded the coal seams and strata along the relevant secondary faults (Figure 1).

2.2. Burial and Geological History of Coal Measuring Strata of Tiefa Basin. As presented in Figure 3, the burial history of the Fuxin Formation in the coal-bearing strata can be roughly divided into six stages. The first stage is early Fuxin Formation−Jurassic−early Cretaceous. During this period, the
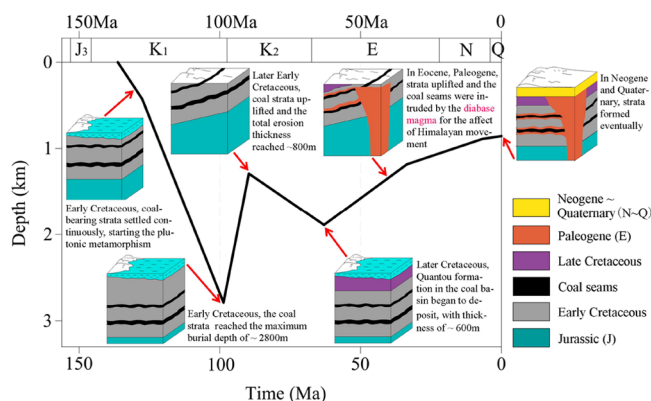
Figure 3. Stratigraphic evolution and burial history of the coal measure strata of Tiefa Basin.

Table 2. Geochemical and Petrographic Analyses of Daxing Coal Samples near Sill/Dike Intrusions[a]

coal seam number	sample	Dis (m)	proximate analysis (wt %)			macerals (vol %)				R_o (%)	T (°C)
			Mois	Ash	VM	V	I	E	M		
9	D1	0.2	3.1	36.6	17.5	97.9	0.9	0.6	0.6	1.14	169
9	D2	0.5	3.4	34.3	21.6	97.1	0.6	0.8	1.5	0.82	127
9	D3	1.0	4.4	20.0	29.0	96.4	1.2	2.1	0.3	0.80	124
9	D4	2.0	4.4	16.0	32.7	96.0	2.1	1.1	0.8	0.74	114
9	D5	3.5	6.3	6.5	36.1	95.2	1.9	0.8	2.1	0.66	99
9	D6	5.0	6.2	4.7	37.0	94.6	2.3	1.4	1.7	0.60	87
9	D7	7.0	6.4	4.7	38.4	93.5	5.7	0.2	0.6	0.56	78
9	D8	10.0	5.8	4.0	37.4	89.9	8.2	0.6	1.3	0.57	80

[a]Dis = distance from sill/dike; Mois = moisture; Ash is on a dry basis; VM = volatile matter; on dry ash free (daf) basis; V = vitrinite, I = inertinite, E = exinite, M = mineral; R_o = random vitrinite reflectance (%, oil); T = maximum paleo temperature.
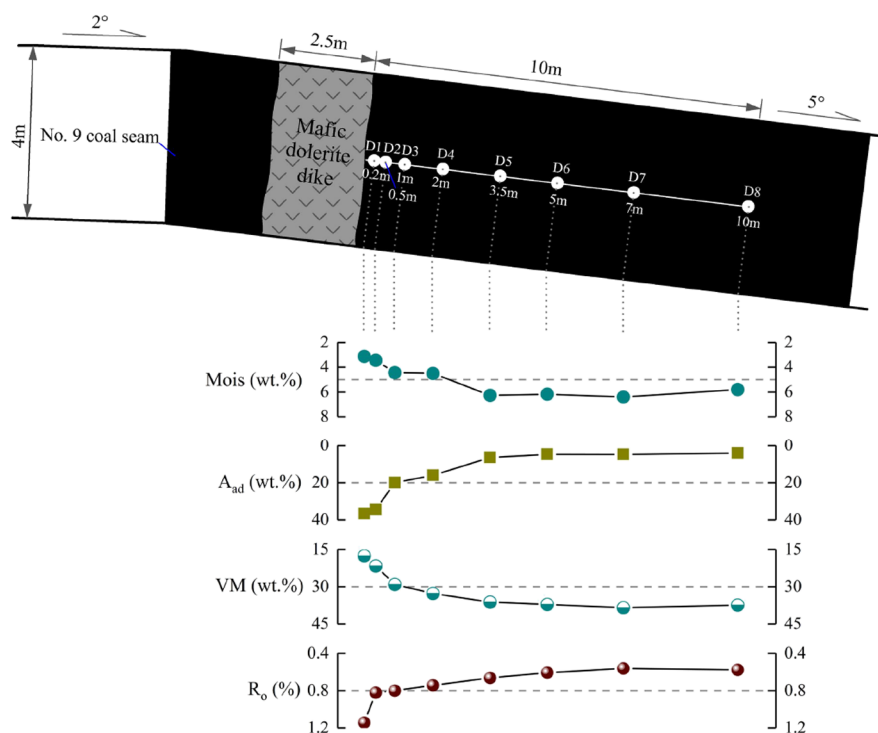
Figure 4. Moisture (Mois), ash (A_{ad}), VM, and vitrinite reflectance (R_o) of coal at different distances from the dike boundary.

in situ stress field dominated by the north−northeast−south−eastern eastward extension of the Tiefa Basin was weakened twice, and the coal seams experienced a deep metamorphic stage. The second stage is late Fuxin Formation−early Cretaceous. During this period, the tensile stress field continued to weaken. The third stage is from late Early Cretaceous to the Upper Cretaceous. During this period, the fault of the western Gangtun fracture was transformed into the reverse fault of the eastern side rising. The fourth stage is the middle and late period of the Late Cretaceous in which most of the basins were deposited with Quantou Formation. The fifth stage is the Tertiary, since Paleogene. During this stage, the Himalayan movement raised the Tiefa Basin as a whole, and a large amount of magma intruded the coal-bearing strata, causing widespread erosion, and the coal-bearing strata were again subjected to erosion and weathering. The sixth stage is the Neogene−Quaternary period during which the surface folds of the basin and the formation of coal-bearing strata eventually formed.

3. METHODOLOGY

3.1. Sample Preparation. To investigate the influence of different occurrence of magma on the porosity, coal rank, and adsorption characteristics of coals, eight coal samples (named D1−D8, 0.2−10 m from the dike) were taken from the No. 9 coal seam in Daxing Mine, Tiefa coalfield.

To study the desorption capacity of coal samples with different moisture contents, 1−3 mm coal particles with different moisture contents were prepared as coal samples. The dry coal samples were weighed and placed in a vacuum tank for vacuum treatment and later weighed again. Then the coal samples were made to absorb water vapor until saturation, and the moisture content of coal was calculated from the change in weight. Then, the saturated water coal samples were evacuated and the moisture content of the coal samples was obtained based on the vacuum time (2.35, 4.52, 6.63, and 8.64%, respectively). Finally, methane gas was introduced into them to achieve adsorption equilibrium. To study the effects of igneous intrusion on the gas and moisture content of coal seams, 20 coal samples at different buried depths were collected from the

No. 4 coal seam (above the sill), the No. 7 coal seam (below the sill), and the No. 12 coal seam (normal) in the Daxing Mine.

3.2. Analytical Methods. According to ASTM standards (ASTM: 2007), the proximate analysis of coal was carried out using a 5E-MAG6600 automatic industrial analyzer. Based on the international standards (ISO 7404-5: 1984), vitrinite reflectance (R_o) was measured using (Zeiss, Germany) a microscope photometer. The maximum paleo temperature (T_{peak}, the coal/intrusion contact temperature) can be calculated by the following formula established by Barker and Pawlewicz:[51]

$$T_{peak} = (\ln(R_o) + 1.19)/0.00782 \qquad (1)$$

Referring to Taylor and Glick,[52] the maceral composition of the coals can be obtained through incident light microscopy and oil immersion. The porosity of the coal was measured by the mercury injection method of Auto Pore IV 9510 (Micromeritics, USA). During the methane adsorption experiment, 50 g crushed coal with a particle size of 0.2−0.25 mm were set at 30 °C, and the adsorption equilibrium gas pressure reached 6 MPa. The determination of gas content adopts the direct method and follows the Chinese national standard (State Administration of Coal Mine Safety of China: 2008). The gas desorption experiment of coal samples with different moisture contents was carried out for 120 min. The gas desorption amount of coal samples with various moisture contents at different times can be obtained by the drainage method.

4. RESULTS AND DISCUSSION

4.1. Influence of Igneous Intrusion on the Geochemistry and Coalification of Bituminous Coal. The moisture, ash, VM, vitrinite, inertinite, exinite, mineral, and vitrinite reflectance of coal samples are listed in Table 2. Approaching the dike, vitrinite increases from 89.9 to 97.9% and inertinite decreases from 8.2 to 0.9%. The change law of exinite and mineral is not obvious. The relationship curves of moisture, ash, VM, and R_o of the coal samples with different distances from the dike are shown in Figure 4.

The range of R_o of the coal samples (D1−D8) at different distances from the dike (about 2.5 m thick) is 0.56−1.14% (Table 2). Based on the international coal classification standard, the eight coal samples are bituminous coals. With decreasing distance to the dike, the R_o increases from 0.56% (D7, 7 m from the dike) to 1.14% (D1, 0.2 m from the dike) (Figure 4). The ash yield gradually increases from 4.02% (D8, 10 m from the dike) to 36.6% (D1, 0.2 m from the dike). The VM content gradually decreases from 38.4% (D7, 7 m from the dike) to 17.5% (D1, 0.2 m from the dike) (Figure 4). The decrease of the VM implies the improvement of coal metamorphic degree, which has a good negative correlation with R_o (Figure 4). According to the variation of R_o, the thermal aureole of the dike is determined to be about 5 m.

T_{peak} of coal seam in the Daxing Coal Mine can be estimated by R_o from formula 1, and the estimated T_{peak} is listed in Table 2. The paleo temperature of No. 9 coal seam near the dike rises from 78 to 169 °C. Therefore, under the thermal evolution of igneous, the paleo temperature of the Daxing Coal Mine heat-affected coal seam increases from ∼78 to ∼169 °C on the whole.

Due to the different background coal rank before igneous intrusion, the influence of igneous intrusion on the coal was obviously different. R_o of coal samples approaching the intrusion of Telkwa coal seam increases from 0.79% (4.2 m from the intrusion) to 7% (0.05 m from the intrusion),[10] which increases 6.21% by igneous intrusion. R_o of the coal samples approaching the intrusion of Raton basin increased from 0.9% (11.25 m from the intrusion) to 4.6% (0.75 m from the intrusion),[16] which increased 3.7% by igneous intrusion. R_o of coal samples approaching the intrusion of the Huainan coalfield increased from 0.87% (4 m from the intrusion) to 5.16% (0.5 m from the intrusion),[53] which increased 4.29% by igneous intrusion. The R_o of coal samples approaching the dike of Tiefa Basin increases from 0.57% (10 m from the intrusion) to 1.14% (0.2 m from the intrusion), which increases 0.57% by igneous intrusion. Although the magma in the Tiefa Basin belongs to the basic magma, the temperature of the basic igneous intrusion can reach ∼1000 °C. The impact of igneous intrusion on the coal samples of the Tiefa Basin is less than that of the coal samples with a higher background coal rank before intrusion. It is probably because the coal samples in the Tiefa Basin were bituminous coal before igneous intrusion. Due to the high moisture content of the bituminous coal, the moisture in the coal can absorb part of the heat of magma, and the heat used to heat coal was relatively reduced.

With decreasing distance to the dike, the moisture content of the coal samples gradually decreases from 6.4% (D7, 7 m from the dike) to 3.1% (D1, 0.2 m from the dike). This is mainly due to the heating of the high-temperature igneous intrusion near the dike, which leads to the gasification of moisture in the coal.

There is a competitive adsorption relationship between the methane and water molecules in the coal matrix. When the moisture decreases, the methane adsorption quantity will increase.[44] Igneous intrusion reduces the moisture of coal in the thermal aureole, so methane replaced the adsorption site of the water molecules, which may theoretically improve the methane content and methane adsorption capacity of the heat-affected coal. In addition, the Tiefa Basin is rich in bituminous coal. The bituminous coal has the characteristics of high natural moisture.[45,54] Igneous intrusion caused the sudden decrease of the moisture in bituminous coal, resulting in the vacancy of the water molecular adsorption site and the significant increase of methane adsorption capacity. In terms of methane adsorption capacity, high-rank coal is less affected by water compared with low-rank coal.[49]

4.2. Influence of Igneous Intrusion on Adsorption/Desorption Properties and Moisture Content. The test results of Langmuir volume (V_L), Langmuir pressure (P_L), and the porosity of coal samples are listed in Table 3.

With decreasing distance to the dike, the porosity of the coal samples increases from 7.7% (D7, 7.0 m from the dike) to 9.4% (D3, 1.0 m) and then decreases to 4.3% (D1, 0.2 m from the dike) (Table 3). The result shows that the porosity of most coal in the thermal aureole increased. The decrease of porosity was probably caused by the frequent cleat and fracture filling by mineral, as well as the strongly decreased mesopore and micropore volumes in the altered zone.[33,55]

The methane isothermal adsorption curve of the coal samples near the dike is shown in Figure 5, which conforms to the Langmuir Model.[56,57] The isothermal adsorption curve increases rapidly in the low-pressure zone (<2000 kPa), and gradually slows down in the high-pressure zone (>4000 kPa)

Table 3. Porosity Characteristics and Methane Adsorption Capacity of Coal Samples[a]

sample	Dis (m)	V_L (m³/t)	P_L (kPa)	porosity (%)
D1	0.2	18.4	827.5	4.3
D2	0.5	23.6	1167.7	7.8
D3	1.0	28.7	977.4	9.4
D4	2.0	25.3	1822.2	8.8
D5	3.5	24.7	1117.3	7.1
D6	5.0	24.4	993.4	8.4
D7	7.0	22.7	999.0	7.7
D8	10.0	23.7	1117.3	na

[a]Dis = distance from sill/dike; V_L = Langmuir volume; P_L = Langmuir pressure; na = not analyzed.
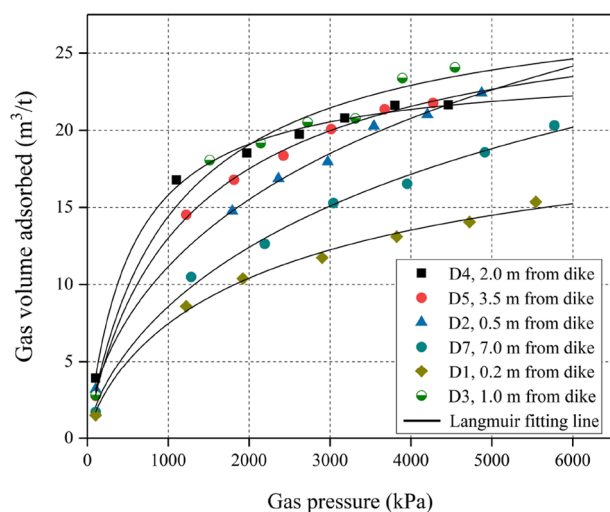
Figure 5. Comparison of methane adsorption behavior and Langmuir fitting lines of six samples.

(Figure 5). With decreasing distance to the dike, the Langmuir volume of the coal sample first increases then decreases. The variation relationship is shown in Figure 6. With decreasing distance to the dike, V_L initially increases from 22.7 m³/t (D7, 7.0 m from the dike) to 28.7 m³/t (D3, 1.0 m from the dike) and then gradually decreases to 18.4 m³/t (D1, 0.2 m from the dike) (Table 3).

The coal in the thermal aureoles had special fractures and micropores. The synergistic effect may improve the methane
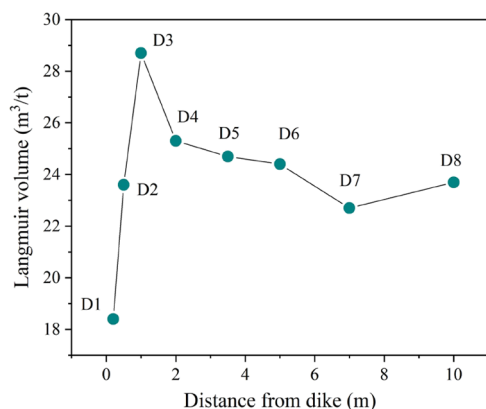
Figure 6. Langmuir volume of the coal seam near a dike in the Daxing Coal Mine.

adsorption capacity, gas desorption, and permeability.[17] Some hydroxyl groups with polar sites on the surface of the coal matrix are more easily occupied by water, which reduces the adsorption capacity of the coal matrix for CH_4 and CO_2. Therefore, the adsorption capacity of wet coal or low-rank coal is significantly lower than that of dry coal or high-rank coal.[45,49,58]

With the increase of R_o, the moisture in heat-affected coal decreases (Figure 7a). A negative linear correlation between the moisture content and R_o was represented. With the decrease of moisture, V_L of the coal generally has an increasing trend, except sample D2 (Figure 7b). There is a linear positive correlation between V_L and R_o in dry coal, and a parabolic (U shape) relationship between V_L and R_o in moisture coals.[45] However, the relationship between moisture and V_L in Figure 7b is relatively discrete, which may be due to the same influence of other factors on V_L. The ash (daf basis) increases dramatically toward the dike, ranging from 4.0 to 36.6% (D8−D1) (Table 2). With decreasing distance to the dike, the porosity first increases from 7.7% (D7, 7 m from the dike) to 9.4% (D3, 1 m from the dike), then decreases to 4.3% (D1, 0.2 m from the dike) (Table 3).

To investigate the effect of moisture content in the coal matrix on gas desorption characteristics, the gas desorption data of four groups of coal samples with different moisture contents (moisture is 2.35, 4.52, 6.63, and 8.64%, respectively) and one group of dry coal samples under the initial equilibrium pressure of 1.00 MPa were measured. After data processing, the 120 min desorption curves of coal samples under different moisture contents were obtained, as shown in Figure 8. The change law of the gas desorption curve of five groups of coal samples is that it tends to be stable after increasing to the limit desorption capacity, which is 5.00, 3.45, 2.31, 1.37, and 0.90 cm³/g, respectively. It is obvious that with the increase of the moisture content of the coal sample, the limit desorption capacity decreases. At the same time, the lower the moisture of coal samples, the faster the early gas desorption rate. Therefore, the coal with a low moisture content has the characteristics of fast gas desorption rate and large amount of gas desorption, resulting in a higher outburst risk than the coal seam with a high moisture content.

4.3. Influence of Igneous Intrusion on the Moisture and Gas Content of Coal Seams. To investigate the influence of sill on gas emission from the coalface during the coal mining process, coal samples were taken in the return airway of coalface N_1408, N_1708, and N_21203 at different depths in Daxing Coal Mine. Twenty coal samples were collected in each coalface with a total of 60 samples. These samples are used to determine the gas content (by direct methods) and moisture (by proximate analysis).

According to the results of borehole exposure, the samples of coalface N_1408 and N_1708 are within twice the thickness of the sill, and there is no igneous intrusion near the coalface N_21203. The determination results of moisture, VM, and gas content of coal samples from three coalfaces are shown in Figure 9a (the data in the figure are from field measurement).

As can be seen from Figure 9a, the moisture content and VM at the sampling points of No. 4 coal seam and No. 7 coal seam in the upper layer are lower than that of No. 12 coal seam in the lower, and the gas content of No. 4 coal seam and No. 7 coal seam is higher than that of No. 12 coal seam. The smaller the VM, the greater the metamorphic degree, which indicates that the metamorphic degree of No. 4 coal seam and No. 7
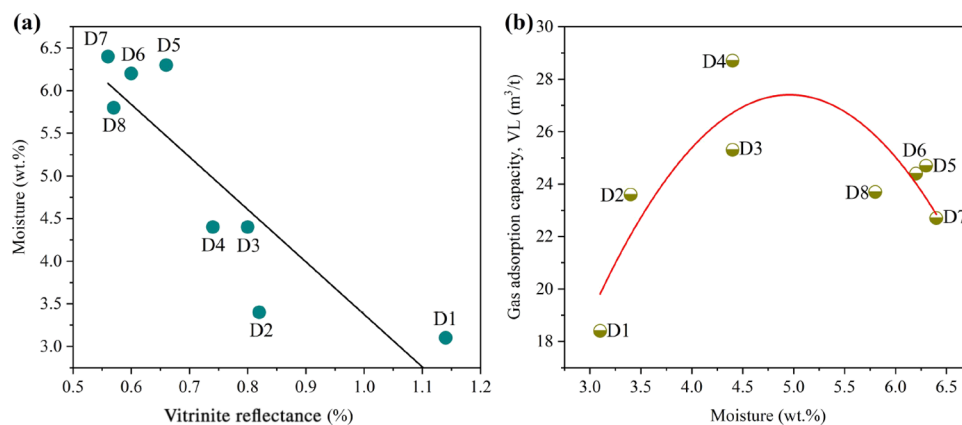
Figure 7. Relationships between moisture and R_o (a) and moisture and Langmuir volume (b) of heat-affected coal samples.
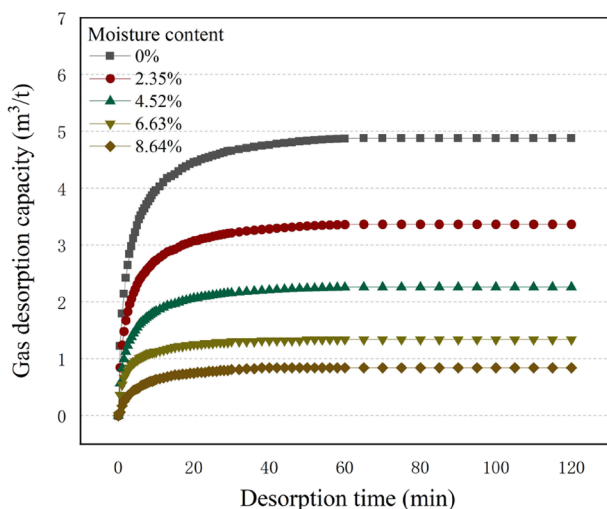
Figure 8. Gas desorption curves of coal samples with different moisture contents in Daxing Coal Mine.

coal seam was improved by thermal evolution. Figure 9b shows the relationship between gas content and moisture in coalface N_1408, N_1708, and N_21203 in the Daxing coalfield. On the whole, with the decrease of moisture content, the gas content of all 60 measuring points in three coal seams significantly increases.

Generally speaking, the deeper the coal seam is buried, the higher the gas content and metamorphic degree are, and the smaller the water content is. The field data of the Tiefa coal mine do not conform to the above law (Figure 9a) because No. 4 coal seam and No. 7 coal seam are located in the upper and lower part of the sill, respectively. In geological history, igneous intrusion is often accompanied by secondary hydrocarbon generation, and the hydrocarbon generation quantity can reach 340 m³/t.[50] Therefore, the gas content of thermal evolution coal seam is usually much higher than that of normal coal seam. At the same time, under the influence of the sill, their metamorphic degree, moisture, and pore properties changed, resulting in a stronger gas adsorption capacity than that of No. 12 coal seam. Jiang et al.[28] found that the abnormally high formation pressure was created by the thermal evolution and trap effect of sill intrusion. Therefore, it can be assumed that the gas content of No. 7 coal seam is higher than that of No. 4 coal seam due to the trap effect of the sill.

Compared to the fitting lines of three coal seams, the fitting line slope of No. 4 coal seam and No. 7 coal seam is higher than that of No. 12 coal seam (Figure 9b). This sequence is
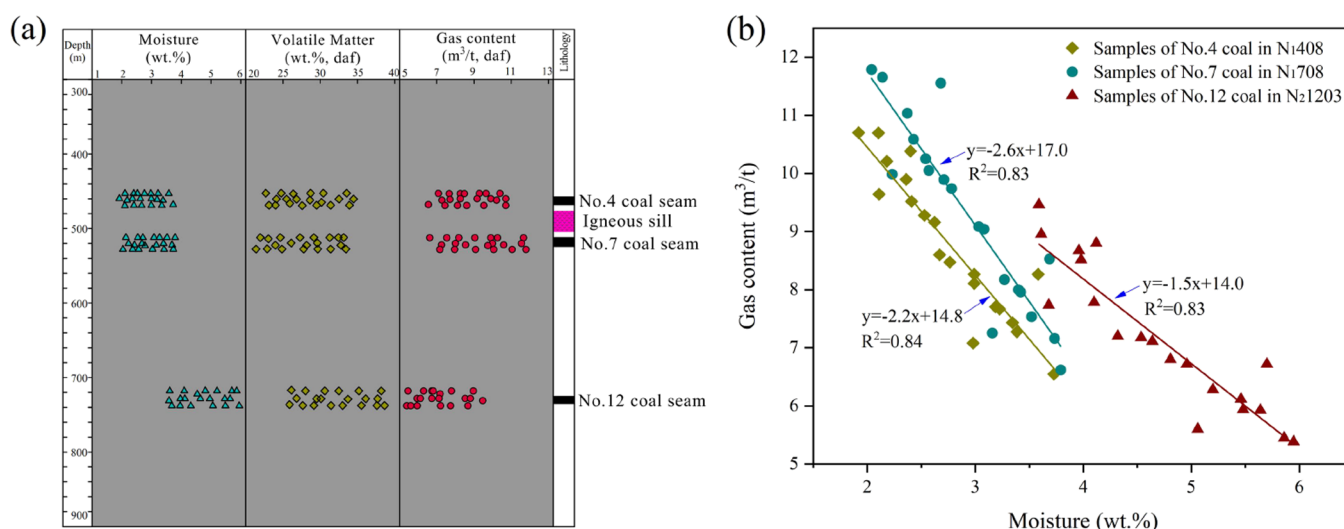
Figure 9. Moisture, volatility, and gas content of three coal seams with different buried depths (a); relationship between the gas content and moisture of the coal samples in the Daxing Coal Mine (b).

completely consistent with the metamorphic degree sequence of the three coal seams. Therefore, it can be inferred that the higher the metamorphic degree, the more obvious the gas content of the coal seam affected by moisture.

4.4. Characteristics of Moisture and Methane Occurrence and Evolution after Igneous Intrusion.

According to the brief burial history of Tiefa Basin (Figure 3), the evolution of CBM can be divided into two stages. At the end of Early Cretaceous, the first hydrocarbon generation (R_o = 0.41−0.45%) was experienced, and Fuxin Formation entered a mature stage. The coal seam was in the stage of uplift in Neogene, and the contact metamorphism of the Himalayan igneous intrusion resulted in the local coal rank elevation and the secondary hydrocarbon generation (R_o = 0.45−0.70%). The uplift stage from the end of Cretaceous to the present was the main stage for the generation of secondary biogenic gas.

Therefore, the CBM reservoir was formed by the first hydrocarbon generation of Yanshanian thermogenesis in Early Cretaceous,[39] and the second hydrocarbon generation of the Himalayan igneous intrusion and continuous biological hydrocarbon generation were the main supplement. Due to the evolution of stratum sedimentation, the moisture and gas in coal seam were significantly affected. The variation of moisture in coal during the sedimentary evolution of coal strata in Daxing Coal Mine is presented in Figure 10.
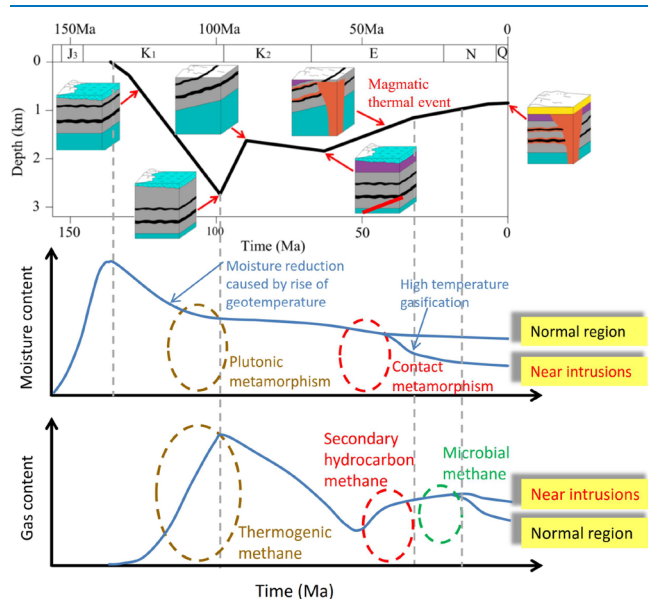
Figure 10. Variation of moisture and gas content of bituminous coal during strata sedimentary evolution.

The moisture content in the coal seam increased rapidly during 140−100 Ma. In the period of 100−65 Ma, because of the rising geotemperature, the moisture content in the coal seam began to show an obvious downward trend, and the downward trend slowed down in the period of 65−55 Ma (Figure 10). From 55 to 40 Ma, due to the influence of contact metamorphism, high-temperature igneous intrusion led to a large amount of water to be gasified, and the moisture content of heat-affected coal was significantly lower than that of unaltered coal (Figure 10). Since 125 Ma, due to deep metamorphism, a large amount of gas has been gradually generated in the coal seam, and the amount of thermogenic methane generated reaches the maximum at 100 Ma (Figure

10). At 100−55 Ma, the coal seam was eroded due to the uplift of the stratum and exposed to the atmosphere, which led to a large amount of gas emission. Therefore, during this period, the gas content in the coal seam decreased sharply, and the gas content decreased to the lowest value at 55 Ma. During the 55−20 Ma period, the gas content in the coal seam gradually increased due to secondary hydrocarbon generation, and began to decrease slowly at 20 Ma (Figure 10).

During the middle period of 60−30 Ma, the igneous intrusion, and the temperature of the coal seam increased. In the thermal evolution area,[28] the metamorphic degree of coal was improved and water was gasified. This allowed the free methane molecules to occupy some of the adsorption sites vacated by the water molecules (Figure 11), which increases
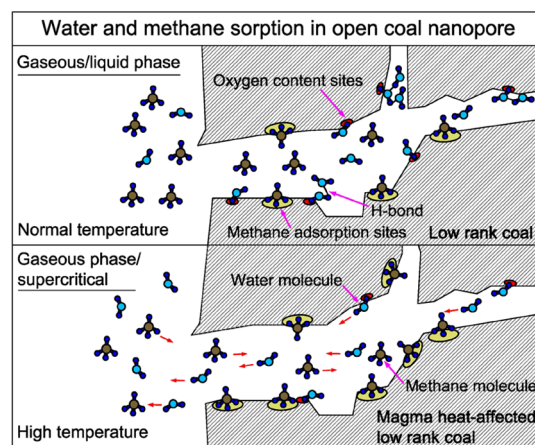
Figure 11. Water and methane sorption in the open nanopore of bituminous coal after igneous thermal evolution.

the overall methane adsorption site on the coal matrix surface. Therefore, the methane adsorption capacity of the heat-affected coal increases (different from the deterioration of the adsorption capacity of the coal samples within 5 m of the intrusion reported by Mastaerz et al.). In addition, the tight roof sill and roof mudstone with good sealing can trap these gases, forming natural gas pockets. This demonstrates that after about 20 Ma, the gas content in the heat-affected coal seam was significantly higher than that of the unaltered coal seam.

5. CONCLUSIONS

In this work, the influence of igneous intrusion on bituminous coal in the Daxing Coal Mine has been systematically analyzed by means of proximate analysis, maceral and R_o determination, isothermal adsorption test, and on-site direct gas content measurement. The main results are as follows:

(1) Approaching the dike (thickness 2.5 m), R_o increased from 0.56 to 1.14% and the moisture content decreased from 6.4 to 3.1%. Under the thermal evolution of igneous intrusion, the paleo temperature of the Daxing Coal Mine heat-affected coal seam increases from ∼78 to ∼169 °C on the whole. Due to the high moisture content of bituminous coal, the coal rank elevation after igneous intrusion is lower than expected.

(2) The thermal evolution of igneous intrusion improves the porosity and adsorption capacity of coal as a whole. It is found that the lower moisture containing coal has faster gas desorption rate and larger gas desorption amount,

resulting in its higher outburst risk than that of higher moisture containing coal.

(3) The gas content of No. 4 and 7 coal seams located at the upper and lower part of the sill is 6.55−10.70 and 7.16−11.79 m^3/t, respectively, which is larger than 5.38−9.47 m^3/t of No. 12 coal seam (the largest buried depth is not affected by sill). The moisture content of No. 4 and 7 coal seams affected by igneous intrusion is 1.92−3.79%, which is less than 3.59−5.95% of No. 12 coal seam. Combined with the VM analysis results, it is concluded that with the decrease of moisture content, the gas content significantly increases.

(4) Due to the rise of geotemperature, the moisture content in the coal seam decreased after 140 Ma, and igneous intrusion exacerbated this phenomenon. During this period, Tiefa Basin experienced two hydrocarbon generation processes, which increased the gas content. After the second hydrocarbon generation, the temperature of coal seam increased with the igneous intrusion, which gasified the water in the coal while improving the gas adsorption capacity of coal. A reasonable explanation is made for the phenomenon that the gas content of heat-affected coal seam is significantly higher than that of unaltered coal seam.

■ AUTHOR INFORMATION

Corresponding Author

Jingyu Jiang − *Key Laboratory of Gas and Fire Control for Coal Mines, Ministry of Education, National Engineering Research Center for Coal Gas Control, and School of Safety Engineering, China University of Mining and Technology, Xuzhou, Jiangsu 221116, China;* orcid.org/0000-0001-9853-7487; Email: jiangjingyu@cumt.edu.cn

Authors

Yiming Huang − *Key Laboratory of Gas and Fire Control for Coal Mines, Ministry of Education, National Engineering Research Center for Coal Gas Control, and School of Safety Engineering, China University of Mining and Technology, Xuzhou, Jiangsu 221116, China*

Yuanping Cheng − *Key Laboratory of Gas and Fire Control for Coal Mines, Ministry of Education, National Engineering Research Center for Coal Gas Control, and School of Safety Engineering, China University of Mining and Technology, Xuzhou, Jiangsu 221116, China;* orcid.org/0000-0002-5109-038X

Huazhou Huang − *School of Resources and Geosciences, China University of Mining and Technology, Xuzhou, Jiangsu 221116, China*

Lei Zhang − *School of Mines, China University of Mining and Technology, Xuzhou, Jiangsu 221116, China*

Complete contact information is available at:
https://pubs.acs.org/10.1021/acsomega.2c06932

Notes

The authors declare no competing financial interest.

■ ACKNOWLEDGMENTS

■ REFERENCES

(1) Tong, Y.; Ibarra, D. E.; Caves, J. K.; Mukerji, T.; Graham, S. A. Constraining basin thermal history and petroleum generation using palaeoclimate data in the Piceance Basin, Colorado. *Basin Res.* **2017**, *29*, 542−553.

(2) Kalinowski, A. A.; Gurba, L. W. Interpretation of vitrinite reflectance−depth profiles in the Northern Denison Trough, Bowen Basin, Australia. *Int. J. Coal Geol.* **2020**, *219*, No. 103367.

(3) Glikson, M.; Boreham, C. J.; Thiede, D. S.Coal Composition and Mode of Maturation, a Determining Factor in Quantifying Hydrocarbon Species Generated. In *Coalbed Methane: Scientific, Environmental and Economic Evaluation*; Mastalerz, M.; Glikson, M.; Golding, S. D., Eds.; Springer: Netherlands, 1999; pp 155−185.

(4) Yao, Y. B.; Liu, D.; Huang, W. Influences of igneous intrusions on coal rank, coal quality and adsorption capacity in Hongyang, Handan and Huaibei coalfields, North China. *Int. J. Coal Geol.* **2011**, *88*, 135−146.

(5) Misra, S.; Varma, A. K.; Hazra, B.; Biswas, S.; Samad, S. K. The influence of the thermal aureole asymmetry on hydrocarbon generative potential of coal beds: Insights from Raniganj Basin, West Bengal, India. *Int. J. Coal Geol.* **2019**, *206*, 91−105.

(6) Gröcke, D. R.; Rimmer, S. M.; Yoksoulian, L. E.; Cairncross, B.; Tsikos, H.; van Hunen, J. No evidence for thermogenic methane release in coal from the Karoo-Ferrar large igneous province. *Earth Planet. Sci. Lett.* **2009**, *277*, 204−212.

(7) Saghafi, A.; Pinetown, K. L.; Grobler, P. G.; van Heerden, J. H. P. CO2 storage potential of South African coals and gas entrapment enhancement due to igneous intrusions. *Int. J. Coal Geol.* **2008**, *73*, 74−87.

(8) Smith, R. M. H.; Eriksson, P. G.; Botha, W. J. A review of the stratigraphy and sedimentary environments of the Karoo-aged basins of Southern Africa. *J. Afr. Earth Sci. (Middle East)* **1993**, *16*, 143−169.

(9) Sachsenhofer, R. F.; Privalov, V. A.; Panova, E. A. Basin evolution and coal geology of the Donets Basin (Ukraine, Russia): An overview. *Int. J. Coal Geol.* **2012**, *89*, 26−40.

(10) Goodarzi, F.; Gentzis, T.; Grasby, S. E.; Dewing, K. Influence of igneous intrusions on thermal maturity and optical texture: Comparison between a bituminous marl and a coal seam of the same maturity. *Int. J. Coal Geol.* **2018**, *198*, 183−197.

(11) Yoksoulian, L. E.; Rimmer, S. M.; Rowe, H. D. Anatomy of an intruded coal, II: effect of contact metamorphism on organic δ13C and implications for the release of thermogenic methane, Springfield (No. 5) Coal, Illinois Basin. *Int. J. Coal Geol.* **2016**, *158*, 129−136.

(12) Rahman, M. W.; Rimmer, S. M. Effects of rapid thermal alteration on coal: Geochemical and petrographic signatures in the Springfield (No. 5) Coal, Illinois Basin. *Int. J. Coal Geol.* **2014**, *131*, 214−226.

(13) Yao, Y.; Liu, D. Effects of igneous intrusions on coal petrology, pore-fracture and coalbed methane characteristics in Hongyang, Handan and Huaibei coalfields, North China. *Int. J. Coal Geol.* **2012**, *96−97*, 72−81.

(14) Sarana, S.; Kar, R. Effect of igneous intrusive on coal microconstituents: Study from an Indian Gondwana coalfield. *Int. J. Coal Geol.* **2011**, *85*, 161−167.

(15) Dai, S. F.; Ren, D. Y. Effects of magmatic intrusion on mineralogy and geochemistry of coals from the Fengfeng-Handan coalfield, Hebei, China. *Energy Fuels* **2007**, *21*, 1663−1673.

(16) Cooper, J. R.; Crelling, J. C.; Rimmer, S. M.; Whittington, A. G. Coal metamorphism by igneous intrusion in the Raton Basin, CO and NM: Implications for generation of volatiles. *Int. J. Coal Geol.* **2007**, *71*, 15−27.

(17) Gurba, L. W.; Weber, C. R. Effects of igneous intrusions on coalbed methane potential, Gunnedah Basin, Australia. *Int. J. Coal Geol.* **2001**, *46*, 113−131.

(18) Qin, Y. J.; Jin, K.; Tian, F. C.; Su, W. W.; Ren, S. K. Effects of ultrathin igneous sill intrusion on the petrology, pore structure and

ad/desorption properties of high volatile bituminous coal: Implications for the coal and gas outburst prevention. *Fuel* **2022**, *316*, No. 123340.

(19) Li, S. K.; Zhu, Y. M.; Wang, Y.; Liu, J. Effects of Rapid Igneous Intrusion Heating on the Geochemistry, Petrography, and Microcrystalline Structure of Coals from Huainan, China. *ACS Omega* **2022**, *7*, 15439−15450.

(20) Chen, H.; Wang, S. Q.; Deng, J. S.; Zhang, X. M.; Liu, Y.; Li, X. G. Petrologic Characteristics and Chemical Structures of Macerals in a Suite of Thermally Altered Coals by Confocal Raman. *ACS Omega* **2021**, *6*, 33409−33418.

(21) Jiang, J. Y.; Zhao, K.; Cheng, Y. P.; Zheng, S. J.; Zhang, S.; Wang, R. Numerical simulation of magma intrusion on the thermal evolution of low-rank coal. *Environ. Earth Sci.* **2021**, *80*, 562.

(22) Finkelman, R. B.; Bostick, N. H.; Dulong, F. T.; Senftle, F. E.; Thorpe, A. N. Influence of an igneous intrusion on the inorganic geochemistry of a bituminous coal from Pitkin County, Colorado. *Int. J. Coal Geol.* **1998**, *36*, 223−241.

(23) Li, K.; Rimmer, S. M.; Liu, Q. Geochemical and petrographic analysis of graphitized coals from Central Hunan, China. *Int. J. Coal Geol.* **2018**, *195*, 267−279.

(24) Saghafi, A.; Faiz, M.; Roberts, D. CO2 storage and gas diffusivity properties of coals from Sydney Basin, Australia. *Int. J. Coal Geol.* **2007**, *70*, 240−254.

(25) Jiang, J. Y.; Cheng, Y. P.*Effects of Igneous Intrusion on Microporosity and Gas Adsorption Capacity of Coals in the Haizi Mine, China*; Scientific World Journal, 2014.

(26) Li, Y.; Zhang, C.; Tang, D. Z.; Gan, Q.; Niu, X. L.; Wang, K.; Shen, R. Y. Coal pore size distributions controlled by the coalification process: An experimental study of coals from the Junggar, Ordos and Qinshui basins in China. *Fuel* **2017**, *206*, 352−363.

(27) Li, Y.; Wang, Z. S.; Tang, S. H.; Elsworth, D. Re-evaluating adsorbed and free methane content in coal and its ad- and desorption processes analysis. *Chem. Eng. J.* **2022**, *428*, No. 131946.

(28) Jiang, J. Y.; Cheng, Y. P.; Wang, L.; Li, W.; Wang, L. Petrographic and geochemical effects of sill intrusions on coal and their implications for gas outbursts in the Wolonghu Mine, Huaibei Coalfield, China. *Int. J. Coal Geol.* **2011**, *88*, 55−66.

(29) Raymond, A. C.; Murchison, D. G. Development of organic maturation in the thermal aureoles of sills and its relation to sediment compaction. *Fuel* **1988**, *67*, 1599−1608.

(30) Salmachi, A.; Rajabi, M.; Reynolds, P.; Yarmohammadtooski, Z.; Wainman, C. The effect of magmatic intrusions on coalbed methane reservoir characteristics: A case study from the Hoskissons coalbed, Gunnedah Basin, Australia. *Int. J. Coal Geol.* **2016**, *165*, 278−289.

(31) Gurba, L. W.; Ward, C. R. Elemental composition of coal macerals in relation to vitrinite reflectance, Gunnedah Basin, Australia, as determined by electron microprobe analysis. *Int. J. Coal Geol.* **2000**, *44*, 127−147.

(32) Guo, Q.; Fink, R.; Littke, R.; Zieger, L. Methane sorption behaviour of coals altered by igneous intrusion, South Sumatra Basin. *Int. J. Coal Geol.* **2019**, *214*, No. 103250.

(33) Mastalerz, M.; Drobniak, A.; Schimmelmann, A. Changes in optical properties, chemistry, and micropore and mesopore characteristics of bituminous coal at the contact with dikes in the Illinois Basin. *Int. J. Coal Geol.* **2009**, *77*, 310−319.

(34) Faiz, M. M.; Saghafi, A.; Barclay, S. A.; Stalker, L.; Sherwood, N. R.; Whitford, D. J.; Flagship, C. E. T. Evaluating geological sequestration of CO2 in bituminous coals: The southern Sydney Basin, Australia as a natural analogue. *Int. J. Greenh. Gas Control* **2007**, *1*, 223−235.

(35) Zhao, L.; Ward, C. R.; French, D.; Graham, I. T. Mineralogy of the volcanic-influenced Great Northern coal seam in the Sydney Basin, Australia. *Int. J. Coal Geol.* **2012**, *94*, 94−110.

(36) Singh, A. K.; Singh, M. P.; Sharma, M.; Srivastava, S. K. Microstructures and microtextures of natural cokes: A case study of heat-affected coking coals from the Jharia coalfield, India. *Int. J. Coal Geol.* **2007**, *71*, 153−175.

(37) Singh, A. K.; Sharma, M.; Singh, M. P. Genesis of natural cokes: Some Indian examples. *Int. J. Coal Geol.* **2008**, *75*, 40−48.

(38) Zhu, Z. M.; Cui, H. Q.; Zhou, J. Y. Coalbed methane system of the cretaceous Sahai Formation in the Fuxin basin. *J. China Univ. Geosci.* **2007**, *18*, 282−284.

(39) Huang, H.; Sang, S.; Miao, Y.; Dong, Z.; Zhang, H. Trends of ionic concentration variations in water coproduced with coalbed methane in the Tiefa Basin. *Int. J. Coal Geol.* **2017**, *182*, 32−41.

(40) Shi, Q.; Qin, B.; Liang, H.; Gao, Y.; Bi, Q.; Qu, B. Effects of igneous intrusions on the structure and spontaneous combustion propensity of coal: A case study of bituminous coal in Daxing Mine, China. *Fuel* **2018**, *216*, 181−189.

(41) Rodrigues, S.; Esterle, J.; Ward, V.; Glasser, L.; Maquissene, T.; Etchart, E. Flow structures and mineralisation in thermally altered coal from the Moatize Basin, Mozambique. *Int. J. Coal Geol.* **2020**, 228.

(42) Jiang, J. Y.; Cheng, Y. P.; Zhang, S. Quantitative characterization of pore structure and gas adsorption and diffusion properties of low-rank coal. *J. China Coal Soc.* **2021**, *46*, 3221−3233.

(43) Jiang, J. Y.; Zhang, Q.; Cheng, Y. P.; Jin, K.; Zhao, W.; Guo, H. J. Influence of thermal metamorphism on CBM reservoir characteristics of low-rank bituminous coal. *J. Nat. Gas Sci. Eng.* **2016**, *36*, 916−930.

(44) Pan, Z.; Connell, L. D.; Camilleri, M.; Connelly, L. Effects of matrix moisture on gas diffusion and flow in coal. *Fuel* **2010**, *89*, 3207−3217.

(45) Busch, A.; Gensterblum, Y. CBM and CO2-ECBM related sorption processes in coal: A review. *Int. J. Coal Geol.* **2011**, *87*, 49−71.

(46) Tao, S.; Chen, S. D.; Tang, D. Z.; Zhao, X.; Xu, H.; Li, S. Material composition, pore structure and adsorption capacity of low-rank coals around the first coalification jump: A case of eastern Junggar Basin, China. *Fuel* **2018**, *211*, 804−815.

(47) Li, Y.; Yang, J. H.; Pan, Z. J.; Tong, W. S. Nanoscale pore structure and mechanical property analysis of coal: An insight combining AFM and SEM images. *Fuel* **2020**, 260.

(48) Jiang, J. Y.; Zhang, S.; Longhurst, P.; Yang, W. H.; Zheng, S. J. Molecular structure characterization of bituminous coal in Northern China via XRD, Raman and FTIR spectroscopy. *Spectrochim. Acta, Part A* **2021**, *255*, No. 119724.

(49) Day, S.; Sakurovs, R.; Weir, S. Supercritical gas sorption on moist coals. *Int. J. Coal Geol.* **2008**, *74*, 203−214.

(50) Wang, Z.; Su, W.; Tang, X.; Wu, J. Influence of water invasion on methane adsorption behavior in coal. *Int. J. Coal Geol.* **2018**, *197*, 74−83.

(51) Barker, C. E.; Pawlewicz, M. J.Calculation of Vitrinite Reflectance from Thermal Histories and Peak Temperatures. In *Vitrinite Reflectance as a Maturity Parameter, ACS Symposium Series, vol. 570*; American Chemical Society, 1994; pp 216−229.

(52) Taylor, G. H.; Glick, D. C.*Organic petrology : a new handbook incorporating some revised parts of Stach's Textbook of coal petrology*; Gebrüder Borntraeger, 1998.

(53) Wang, R.; Liu, G. Variations of concentration and composition of polycyclic aromatic hydrocarbons in coals in response to dike intrusion in the Huainan coalfield in eastern China. *Org. Geochem.* **2015**, *83−84*, 202−214.

(54) Guo, H.; Cheng, Y.; Wang, L.; Lu, S.; Jin, K. Experimental study on the effect of moisture on low-rank coal adsorption characteristics. *J. Nat. Gas Sci. Eng.* **2015**, *24*, 245−251.

(55) Li, Y.; Wang, Z. S.; Pan, Z. J.; Niu, X. L.; Yu, Y.; Meng, S. Z. Pore structure and its fractal dimensions of transitional shale: A cross-section from east margin of the Ordos Basin, China. *Fuel* **2019**, *241*, 417−431.

(56) Langmuir, I. The Adsorption of Gases on Plane Surfaces of Glass, Mica and Platinum. *J. Am. Chem. Soc.* **1918**, *40*, 1361−1403.

(57) Ye, J. C.; Tao, S.; Zhao, S. P.; Li, S.; Chen, S. D.; Cui, Y. Characteristics of methane adsorption/desorption heat and energy with respect to coal rank. *J. Nat. Gas Sci. Eng.* **2022**, *99*, No. 104445.

(58) Chen, X. J.; Wang, X. D.; Zhao, S.; Kang, N. N.; Feng, S. L. Effect of Moisture on Methane Adsorption Characteristics of Long-Flame Coa. *ACS Omega* **2022**, *7*, 16670−16677.